Polymer Journal (2012) 44, 65–71

www.nature.com/pj

ORIGINAL ARTICLE

Critical roles of molecular dynamics in the superior mechanical properties of *isotactic*-poly(1-butene) elucidated by solid-state NMR

Toshikazu Miyoshi[1] and Al Mamun[2]

***Isotactic*-poly(1-butene) (iPB1) shows superior mechanical properties after crystal–crystal transitions. Recently, Miyoshi *et al.* found that crystalline stems in metastable tetragonal crystal perform uniaxial rotational diffusions accompanying side-chain conformational transitions in the fast motional limit (correlation time, $\langle \tau_c \rangle < 10^{-7}$ s; *Macromolecules* 2010, 43, 3986–3989.). In this study, molecular dynamics in stable trigonal crystal is investigated by solid-state nuclear magnetic resonance, which indicates that crystalline stems and side-chain conformations are completely fixed up to melting points ($\langle \tau_c \rangle > 10$ s). In addition, lamellar thickness, $\langle l \rangle$ of iPB1 and a low isotacticity iPB1 (low_iPB1) with $\langle mmmm \rangle = 78\%$, respectively, were investigated by small-angle X-ray scattering. The low_iPB1 sample shows very week supercooling dependence of $\langle l \rangle$ (~ 5 nm), whereas iPB1 shows strong supercooling dependence of $\langle l \rangle$ (10–28 nm). On the basis of molecular dynamics and $\langle l \rangle$ results, molecular dynamics effects on structures and unique mechanical property of iPB1 are discussed.**
Polymer Journal (2012) **44,** 65–71; doi:10.1038/pj.2011.66; published online 10 August 2011

Keywords: crystal–crystal transition; crystallization; *isotactic*-poly(1-butene); mechanical property; molecular dynamics; solid-state NMR

INTRODUCTION

Isotactic poly(1-butene) (iPB1) is an industrially significant material because of its outstanding mechanical strength compared with chemically similar polyolefins, such as polyethylene (PE), *isotactic*-poly(propylene) (iPP) and *isotactic*-poly(4-methyl-1-pentene) (iP4M1P).[1] In addition to having four polymorphs (I, I′, II and III),[2–5] iPB1 shows complex solid–solid transitions.[6–10] As the samples crystallize from a melt in stationary conditions, a metastable tetragonal crystal of 11_3 helices (form II) is kinetically favored. This form II spontaneously transforms into a stable trigonal crystal of 3_1 helices (form I) at ambient temperature via a solid–solid transition.[6–10] As a result, the bulk mechanical and physical properties are enhanced. These effects are caused neither by an increased crystallinity of the material, because the crystal fraction does not change during the transition, nor by variations of morphology.[11–14] Despite many structural investigations of the solid–solid transition of iPB1,[6–14] the origin of its outstanding mechanical properties is not fully understood.

The molecular dynamics of polymers are highly related to chain packing and available spaces. Solid-state nuclear magnetic resonance (NMR) has been successfully applied to reveal the molecular dynamics of solid polymers in the amorphous and crystalline regions.[15–20] In the crystalline regions, the molecular dynamics of typical polyolefins such as PE,[16] iPP[17,18] and iP4M1P[19] were investigated by two- and one-dimensional exchange NMR, which can directly detect reorientations of magnetic anisotropic interactions that are due to molecular dynamics.[15] These crystalline polymers commonly display slow, helical jump motions in the crystalline regions, which include discrete jump motions around the chain axes and translations of overall stems by one monomer unit. It was indicated that such overall motions in the crystalline region have important roles in crystallization, surface melting, mechanical properties and drawability.[20]

There are several solid-state NMR works on iPB1.[21–27] Maring *et al.*[22] using ^{1}H second moments, detected reduced mobility of iPB following solid–solid transitions. Beckham *et al.*[24] detected overall segmental motions in form II above $T_g = -23\,^\circ$C. Maring *et al.*[23] investigated molecular dynamics in form I using high-resolution ^{13}C NMR. They did not observe any evidence for molecular dynamics in form I in the mid 10 kHz range up to 90 °C. However, the detailed dynamic geometry and time-kinetic parameters of iPB1 have not yet been reported.

Very recently, Miyoshi *et al.*[25,26] revealed using ^{1}H–^{1}H dipolar patterns that crystalline stems in form II undergo continuous rotational diffusion around the chain axis, concomitant with lateral conformational transitions in the fast motional limit (correlation time, $\langle \tau_c \rangle < 10^{-7}$ s) at 100 °C. These dynamic characters are direct evidences for dynamically, conformationally disordered crystals.[28]

[1]Department of Polymer Science, The University of Akron, Akron, OH, USA and [2]Research Institute of Nanotechnology, National Institute for Advanced Industrial Science and Technology, Tsukuba, Ibaraki, Japan
Correspondence: Professor T Miyoshi, Department of Polymer Science, The University of Akron, Goodyear Polymer Center 723, Akron, OH 44325-3909, USA.
E-mail: miyoshi@uakron.edu
Received 5 April 2011; revised 19 May 2011; accepted 22 May 2011; published online 10 August 2011

In this work, we will investigate the molecular dynamics of the stable form I of iPB using center band-only detection of exchange (CODEX)[29] and modified wide-line separation NMR.[30–32] As a result, it is found that crystalline stems in form I do not undergo any overall or side-chain motions, which reorient the principle axes of chemical shift anisotropy (CSA) up to T_m. On the basis of dynamics results in this and previous works,[26] we will discuss the relationship between chain packing and the molecular dynamics of forms I and II. In addition, we will investigate how chain mobility influences the lamellar thickness, $\langle l \rangle$, of iPB1. Here we will use two samples of iPB1 and low *isotactic* PB1 (low_iPB1) ($\langle mmmm \rangle$=78%). Very recently, De Rosa *et al.*[33] found that low tacticity iPB bypasses crystallization into form II and directly crystallizes into the trigonal form (form I′). The two iPB1 samples used in this study display different crystallization mechanisms (through or bypassing form II). Thereby, we demonstrate that the lamellar thickness of iPB1 is highly dependent on the crystalline mobility. Through information about molecular dynamics and the $\langle l \rangle$–$1/\Delta T$ data obtained in this study, we conclude that unique crystallization and irreversible solid–solid transitions dominate the outstanding mechanical properties of iPB1.

EXPERIMENTAL PROCEDURE

Samples

Two samples of iPB1 and one of iPP were used in this work. iPB1, with an average molecular weight of M_w=186 000, a polydispersity of M_w/M_n=3.3 and an isotacticity of $\langle mmmm \rangle$=92%, was purchased from Polysciences Inc. (Warrington, PA, USA). iPB, with a low isotacticity of $\langle mmmm \rangle$=78% and an average molecular weight of M_w=280 000, was kindly provided by Idemitsu Ltd (Sodegaura, Japan). The low isotacticity sample will be referred to as low_iPB. The low_iPB1 was used for investigating $\langle l \rangle$. *i*PP, with an average molecular weight of M_w=360 000, a polydispersity of M_w/M_n=3.3 and an isotacticity of $\langle mmmm \rangle$=97%, was purchased from Polyscience Inc.

We did not further purify any of the samples. The samples were melted between two cover glasses on a hot stage. The thickness of each sample was controlled to be 0.2 mm by inserting a metal spacer between the cover glasses. Each sample was first melted and then crystallized several times to erase the previous thermal history. In a typical experiment, the samples of iPB1 were melted for 5 min at 150 °C. The samples were then rapidly transferred to another hot stage that was preset to a required crystallization temperature, T_c, to allow for isothermal crystallization under nitrogen atmosphere. The sample was completely solidified, and full crystallization was confirmed by polarized optical microscopy. The equilibrium melting temperatures, T_m^0, of iPB and low_iPB were determined to be 135 ± 2 and 90 ± 1 °C, respectively, in terms of a Hoffman–Weeks plot using T_c and T_m obtained using differential scanning calorimetry (DSC). iPP samples were crystallized at 150 °C.

Nuclear magnetic resonance

The ^{13}C solid-state NMR experiments were performed using a Bruker Avance 300 spectrometer (Bruker, Rheinstetten, Germany) equipped with a 4 mm cross polarization magic-angle spinning (CPMAS) NMR probe. The ^1H and ^{13}C carrier frequencies were 300.1 and 75.6 MHz, respectively. The MAS frequency was set to 4000 ± 3 Hz. The 90° pulses for ^1H and ^{13}C were 4.5–5.0 μs. The recycle delay and cross-polarization time were 2 s and 1 ms, respectively. High-power ^1H two-pulse phase modulation decoupling with a field strength of 65 kHz was used over an acquisition time of 80 ms. The chemical shift was referenced to the CH signal of adamantine (29.5 p.p.m.) as an external reference. A phase-sensitive ^1H–^{13}C two-dimensional wide-line separation NMR spectrum was obtained in time-proportional phase increment (TPPI) mode. The data matrix had 512 points along the t_2 dimension and 128 points along the t_1 dimension, with a dwell time of 2 μs. A short cross-polarization of 50 μs was used for the polarization transfer step. Continuous-wave decoupling with a field strength of 55 kHz was applied in the t_1 dimension to suppress ^1H–^{13}C heteronuclear interaction.[26,31,32] The temperature in the sample was carefully calibrated using the temperature dependence of the ^{207}Pb chemical shift of $Pb(NO_3)_2$.[34]

The CODEX experiments use the recoupling of the CSA interaction using 180° pulse trains in the two evolution periods sandwiching a mixing period, t_{mix}.[29] The effect is a signal decay due to the dephasing of the magnetization brought about by changes in the orientation-dependent CSA that results from a reorientational dynamic process during t_{mix}. The magnetization evolves during the initial evolution period, $Nt_r/2$ (where N=2, 4, 6 and so on), under the orientation-dependent CSA interaction, which is recoupled by two successive 180° pulses per MAS rotation period, t_r. The magnetization after the first evolution period is stored along the z direction by a 90° pulse and does not dephase during t_{mix} (which must be set to an integer multiple of t_r). The magnetization evolves again after the 90° readout pulse during the second evolution period ($Nt_r/2$) and is refocused at its end. The second mixing period, t_z, serves as a z-filter and permits the cancellation of longitudinal relaxation. In our experiments, t_z was set to one t_r. Following the last 90° pulse, the signal was detected under ^1H two pulse phase modulation decoupling. If there is no molecular motion during t_{mix}, the evolutions in the two evolution periods will cancel each other out, and there will be no decay of the signal intensity. If there is molecular motion during t_{mix}, the orientation-dependent frequency before and after t_{mix} will be different, and the magnetization will not be completely refocused. The resulting dephasing leads to a decay of the signal intensity in the exchange spectrum (S). To remove the T_1 and spin–spin relaxation (T_2) effects during t_{mix} and Nt_r, a reference spectrum is acquired. It can be obtained simply by interchanging t_{mix} and t_z. The signal intensity in the reference spectrum (S_0) is not sensitive to exchange processes but is only dominated by T_1, T_2 and pulse length errors. The motional correlation time and information about the motional geometry can be obtained by plotting the ratio (S/S_0) versus t_{mix} and (S/S_0) versus Nt_r, respectively. A more detailed description of the CODEX experiment can be found in deAzevedo *et al.*[29] The MAS frequency was 4000 ± 3 Hz. The ^1H radio frequency (rf) field strength for continuous-wave decoupling during the ^{13}C 180° pulse with a pulse length of 15 μs was set to 100 kHz. All other rf parameters were the same as for the CPMAS experiments. The reference and exchange measurements were obtained alternatively every 128 transients to suppress drift of the NMR spectrometer. The $T_{1\rho H}$ filter was incorporated into the CODEX pulse program for suppression of the amorphous signal contribution to the CODEX results at ambient temperature and at −10 °C. In total, each spectrum was obtained by accumulating 1024 transients. The total experimental time for the measurement of the mixing time dependence up to 4 s was approximately 24 h. The total experimental time of a typical Nt_r experiment was approximately 12 h.

Small angle X-ray scattering

Small angle X-ray scattering studies were performed using a CuKα radiation generated by a Rigaku Ultrax 4153A 172B X-ray diffractometer (Rigaku, Akishima, Japan) and a point-focusing small angle X-ray scattering camera. The camera length used was 740 mm, and the images were recorded using an image plate with an exposure time of 2.5 h. Digitized data were then read from the image plate using the image plate reader. Using image plate, very small changes in small angle X-ray scattering patterns could be observed with a very short exposure time. The corrected pattern of an empty sample holder was subtracted from each pattern. To calculate the long period and the lamellar thickness, a correlation function method by Rigaku R-axis software (Rigaku) was used.

Differential scanning calorimetry

All of the samples were measured with an updated computer interfaced Perkin-Elmer DSC-7 (Perkin-Elmer, Waltham, MA, USA). Both temperature and heat-flow levels were corrected by standard materials. Measurements of the melting points were performed at a heating rate of 10 °C min^{-1}. To prevent thermal degradation, nitrogen gas was circulated around the sample pan.

RESULTS AND DISCUSSION

Molecular dynamics in form I

Figure 1 shows ^{13}C CPMAS NMR spectra of iPB1 crystallized at 100 °C, signal assignments and a DSC chart. The T_m of this sample is 130 °C. At ambient temperature, the ^{13}C crystalline signals of form I are very sharp and dominate the spectrum. Very broad signals with

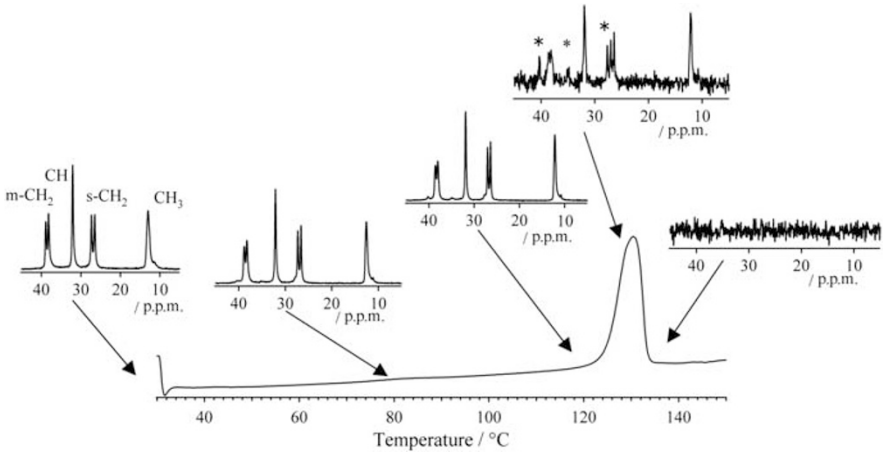

Figure 1 The ^{13}C CPMAS nuclear magnetic resonance spectra of the form I-rich sample of *isotactic*-poly(1-butene) at ambient temperature, 99, 118, 129 and 136 °C, the signal assignments and the differential scanning calorimetry chart. Asterisks indicate the amorphous signals.

very low intensities appear at the bottom of the sharp crystalline signals. These are amorphous components. There are two reasons for broadening in the amorphous signals: structural disorders such as conformations and packings or a dynamic effect. The T_g of iPB1 is −23 °C. Thus, the dynamics frequency of thermally activated ^{13}C amorphous segmental motions reaches the mid 10 kHz order at ambient temperature. If molecular dynamics reaches the ^1H dipolar decoupling (DD) frequency (65 kHz in our experiment), maximum line broadening occurs in the spectrum. This interference effect leads to broadened amorphous signals. The side-chain and main-chain methylene (s-CH and m-CH_2, respectively) carbons in the crystalline regions display doublet signals. Stereoregular polymers can adopt right- or left-handed helical chains. In addition, lateral groups have upward and downward orientations. This orientation disorder provides different atomic positions in s-CH_2 and m-CH_2 carbons and leads to doublet signals (packing effect).[2,23]

At elevated temperature, the ^{13}C line widths of the crystalline signals are almost invariant. Above 99 ± 2 °C, narrowed amorphous signals (indicated by asterisks) appear in the spectra. At 128 ± 2 °C, the crystal is mostly melted and only small crystalline signals and further narrowed amorphous signals are observed. At 136 ± 2 °C, there is no ^{13}C CPMAS signal, indicating complete melting. Through this temperature dependence, ^{13}C line widths of all of the crystalline signals show no broadening up to T_m. This result indicates that molecular dynamics in the crystalline region (except for CH_3 rotation) do not reach the mid 10 kHz range up to T_m.

Figure 2a shows the ^1H MAS NMR spectrum for the form I-rich sample of iPB1 at 118 °C. The spectrum is dominated by a very sharp ^1H signal corresponding to the amorphous component. The ^1H spectrum amplified vertically by a factor of 20 is shown in Figure 2b. This amplified spectrum clearly shows signals for both the crystalline and the amorphous components. To observe functional ^1H line shapes in the crystalline signals, the ^1H–^{13}C wide-line separation spectrum of the form I-rich sample was obtained. Here CP time of 50 μs was used to suppress the spin-diffusion effect.[26,31] In addition, ^{13}C DD during the t_1 detection period was applied to eliminate ^1H–^{13}C heteronuclear dipolar interactions.[31,32] These two modifications provide short range ^1H–^1H dipolar interactions that reflect the local mobility on functional levels. Figures 2c and d show ^1H slice spectra in the main and side chains, respectively, obtained through the highly resolved ^{13}C signals. The obtained line shapes were fitted using Gaussian functions. The best fitted results indicate that ^1H full-line width at half height is

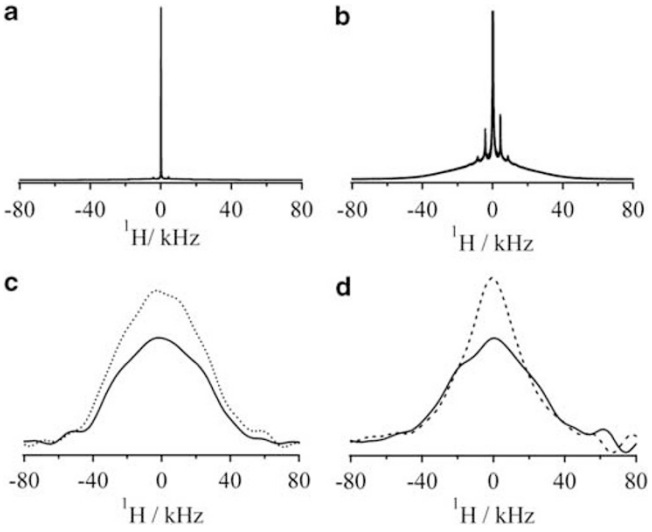

Figure 2 (**a**) Whole and (**b**) ^1H MAS nuclear magnetic resonance spectrum amplified vertically by a factor of 20 and ^1H slice date of ^1H–^{13}C MAS wide-line separation nuclear magnetic resonance spectra of (**c**) the main chains and (**d**) the side chains of the form I-rich sample at 118 °C. The dotted lines show the ^1H slice date through ^{13}C CH and CH_3 signals, and the solid lines show the ^1H ones through ^{13}C m-CH_2 and s-CH_2 signals.

57, 57, 54 and 37 kHz, for m-CH_2, CH, s-CH_2 and CH_3 protons, respectively. The small ^1H full-line width at half height for CH_3 protons is attributed to fast rotations of the CH_3 groups in the crystals. The other ^1H line shapes are the typical rigid ones of solid polymers. This means that the overall and side-chain conformations in form I do not undergo large amplitude motions over a ^1H line width of ∼50 kHz at 118 °C. The small reduction of the ^1H line width of s-CH_2 compared with that of m-CH_2 may be attributed to librational motions of the side chain. This observation is consistent with the former ^{13}C T_1 reduction of s-CH_2 carbon.[23]

To further investigate the slow molecular dynamics in form I crystals, we applied CODEX measurements to iPB1. This method can evaluate slow dynamics in a frequency range of 10^{-1} to 10^3 Hz. This method probes the reorientation of the CSA principle axis directions, which are fixed on ^{13}C atoms due to molecular dynamics. Before investigating the molecular dynamics of iPB1, our pulse

program was tested using iPP, for which the crystalline stems perform helical jump motions with a jump angle of 120° at temperatures above 90 °C.[17,18] The structure and dynamics are shown in Figure 3a. Several works evaluated helical jump motions using the CODEX method.[18,19,29]

Figure 3b shows the Nt_r dependence of the CODEX (S/S_0) for all of the functional signals of the α_2-rich form[18] of iPP with a t_{mix} of 200 ms at 112 °C. The (S/S_0) intensity ratios of all of the signals decay with increasing Nt_r. This means that all of the functional signals participate in molecular dynamics. The decay curve of each carbon relies on the dynamic geometry, the CSA principle axis values and the orientations. The helical jump effects (a jump angle, φ=120°) on CH_2 carbon was numerically simulated, and the simulated result is shown as a solid curve in Figure 3b. Here the CSA size and principle axis orientations reported by Nakai *et al.*[35] were used for simulation. This simulation result reproduces the experimental (S/S_0) decay curves well. This confirms that our CODEX pulse program properly works to evaluate molecular dynamics.

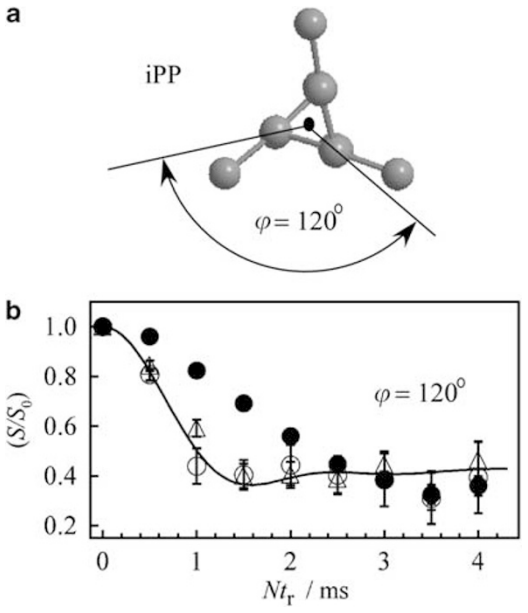

Figure 3 (**a**) The 3_1 helix of the *isotactic*-poly(propylene) (iPP) crystalline stem and the jump angle of the 3_1 helix (φ=120°). (**b**) Center bands only detection of exchange Nt_r dependence of (S/S_0) for the CH_2 (○), CH (●) and CH_3 (Δ) of the *isotactic*-poly(propylene) α_2-rich form with t_{mix}=200 ms at 114 °C. The solid curve shows a simulated result for a helical jump with a jump angle of 120° on CH_2 carbon.

Figures 4a show the CODEX reference (S_0), exchange (S) and difference spectra (S_0–S) of the iPB1 form I with t_{mix}=200 ms and Nt_r=2 ms at ambient temperature. The result clearly indicates that S_0–S is nearly zero in all of the functional signals. The CSA principle axis values of all of the functional signals in iPB1[36] are very similar to other polyolefins.[25,35] Thus, this result demonstrates that there is no large amplitude motion in iPB1 during t_{mix}=200 ms at ambient temperature. ^{13}C–^{13}C spin diffusion also leads to an (S/S_0) decay curve at a longer t_{mix} of more than 1 s even in natural abundance. Thus, spin diffusion correction is necessary to investigate slow dynamics at any t_{mix} longer than 1 s.[19]

Figures 4b and c show the t_{mix} dependence of the $(S/S_0)^*$ intensity ratios of m-CH_2, CH and CH_3 at ambient temperature and at 118 °C, respectively, where asterisk (*) represents the pure CODEX (S/S_0) decay after spin-diffusion corrections. The spin-diffusion effect, $(S/S_0)_{SD}$, was obtained at −10 °C, where no motion is expected. $(S/S_0)^*$ is described in terms of $(S/S_0)/(S/S_0)_{SD}$. The $(S/S_0)^*$ intensity ratios of m-CH_2 and CH carbons do not decay up to t_{mix}=4 s at a fixed Nt_r=2 ms at ambient temperature. The $(S/S_0)^*$ ratios of the CH_3 signal at $t_{mix} \geqslant 2$ s are fluctuated and show large experimental errors. This is caused not by molecular dynamics but by a short ^{13}C T_1 value. At 118 °C, the (S/S_0 (t_{mix}))* intensity ratios of all of the functional signals show similar behaviors to those at ambient temperature. The t_{mix} dependence of the CODEX (S/S_0) intensity ratios is analyzed in terms of $(S/S_0)^*$=

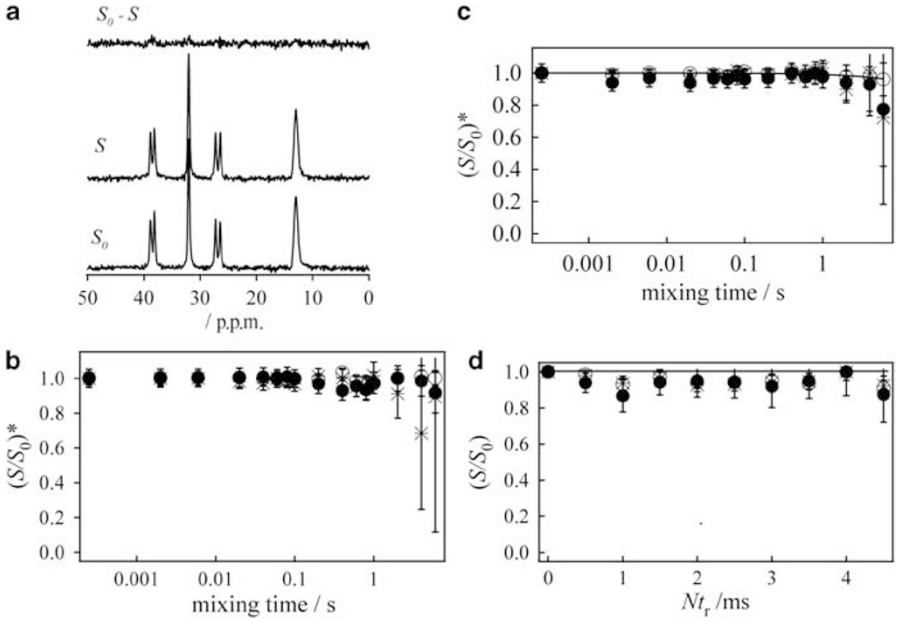

Figure 4 (**a**) The ^{13}C center bands only detection of exchange reference, exchange and difference spectra for the *isotactic*-poly(1-butene) form I at a mixing time of 200 ms and Nt_r=2.0 ms at ambient temperatures. (**b**, **c**) Center bands only detection of exchange t_{mix} dependence of $(S/S_0)^*$ and (**d**) Nt_r dependence of the (S/S_0) intensity ratios for m-CH_2 (●), CH (○) and CH_3 (*) with Nt_r=2 ms at (**b**) ambient temperature and at (**c**, **d**) 118 °C.

$1-a(1-\exp(-(t_{mix}/\langle\tau_c\rangle)^{\beta}))$,[29] where a is related to the available site number, p and β is the distribution width. Even at 118 °C, no essential reduction in the $(S/S_0)^*$ intensity ratios was observed up to t_{mix}=4 s. Figure 4c shows the best-fit solid curve with $\langle\tau_c\rangle$=860 ± 5000 s for the experimental data of CH. This long value is outside of the dynamic window in our experiments ($\leqslant$10 s). In this case, the fitted parameters to the experimental data no longer show physical meaning.

In the t_{mix} experiment, Nt_r was fixed to be 2 ms. This value is a typical condition to characterize large amplitude motions of the crystalline segments. In former works, helical jump motions of iPP and iP4M1P were analyzed using Nt_r=2 ms.[18,19] Thus, the current CODEX result denies the presence of large amplitude motions in iPB1 form I in the slow dynamic range even at very high temperatures just before T_m. If iPB1 may have small amplitude motions, the decay curve requires a longer Nt_r to detect the molecular dynamics. Figure 4d shows the Nt_r dependence of the (S/S_0) intensity rations for m-CH_2, CH and CH_3 ^{13}C signals with t_{mix}=200 ms at 118 °C. The (S/S_0) intensity ratios of all of the signals do not decay with increasing Nt_r up to 4.5 ms. The solid line in Figure 4d represents a jump angle of 0°, which is consistent with the experimental results within the error. This means there is essentially no molecular dynamics in both the main and the side chains in the slow dynamic range. Thus, the dependence of both the t_{mix} and the Nt_r on the CODEX experiments indicates that there are no overall or side-chain motions that induce reorientations of the CSA principle axes of all of the functional signals of form I up to T_m. These dynamics results are consistent with the results of ^{1}H line widths and ^{13}C line widths under DD.

Further, the molecular dynamics of form I′ was also investigated using the ^{13}C line width under DD and CODEX. The ^{13}C line widths under DD were invariant up to the melting point (78 °C). The CODEX Nt_r dependencies of m-CH_2, CH and CH_3 signals with t_{mix}=200 ms at 75 °C are shown in Figure 5. None of the signals display a decay up to Nt_r=4.5 ms. The CODEX t_{mix} dependencies of all of the signals with Nt_r=2 ms at 75 °C also indicate no decay of any of the signals up to t_{mix}=4 s (data are not shown). These experimental results indicate that, although there is a significant difference in the melting points between forms I and I′, the dynamics characteristics of form I′ are very similar to that of form I.

iPB1 versus other crystalline polymers

Time-kinetic parameters and the geometry of molecular dynamics reflect on their own conformations and chain packing with neighboring molecules (available dynamic space). Our previous results revealed that the crystalline stems in form II undergo uniaxial rotational diffusion along with the side-chain conformational transitions in the fast motional limit ($\langle\tau_c\rangle$ $<10^{-7}$ s) at 100 °C.[26] Following the subsequent solid–solid transition, the molecular dynamics drastically changes from fast-limit overall dynamics to no overall dynamics on the NMR time scale (>10 s). This solid–solid transition also accompanies a drastic change in the side-chain dynamics from a fast-limit conformational transition to no transition (>10 s) even at a temperature close to T_m. These drastic mobility changes, both overall and in the side chains, should be simply related to available spaces in the crystalline field. According to crystallographic data,[2,3] the solid–solid transition leads to 15% contraction in the *ab* plane and 12% extension along the *c* axis (chain axis). Such densification leads to a huge dynamic gradient between forms II and I.

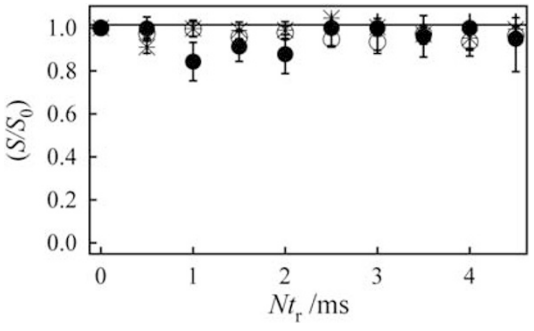

Figure 5 The ^{13}C center bands only detection of exchange reference Nt_r dependence of the (S/S_0) intensity ratios for m-CH_2 (●), CH (○) and CH_3 (*) of low isotacticity *isotactic*-poly(1-butene) with t_{mix}=2 ms at 75 °C just before the onset of melting (78 °C). The solid line represents a jump angle of 0° around the helical axis.

Here it would be interesting to compare the geometry and the time-kinetic parameters of the molecular dynamics observed in forms I and II with those of similar polyolefins. PE (orthorhombic),[16] iPP (α2 form)[17,18] and iP4M1P (form I)[19] commonly show helical jump motions in the crystalline regions. The helical jump motion accompanies jump rotations of overall stems to neighboring sites and translation of overall stems by one monomer unit. Such discrete jump motions are attributed to a well-defined periodicity of chain conformations and packings in the crystalline regions. With regard to the time-kinetic parameters of these dynamics, $\langle\tau_c\rangle$ of the helical jump motions of PE, iPP and iP4M1P were estimated to be 10^{-5}, 5×10^{-2} and 8×10^{-4} s, respectively, at 118 °C using reported activation energies and correlation times.[16,18,19] Though the dynamic geometries are different, it is understood that both the overall dynamics in form II ($\langle\tau_c\rangle$ $<10^{-7}$ s) and the absence of overall motions in form I ($\langle\tau_c\rangle$ >10 s) at 118 °C are much faster and slower, respectively, than $\langle\tau_c\rangle=10^{-2}$–$10^{-5}$ s of the helical jump of three polymers at 118 °C. Therefore, it is understood that the dynamic characteristics (geometry and kinetics) of both forms of iPB1 are largely different from those of similar polyolefins.

Similar types of molecular dynamics (geometry and kinetics) to those in form II were observed in other conformationally disordered crystals such as PE in the hexagonal phase under high pressure[37] and 1,4-*trans*-polybutadiene in the high temperature phase.[38] Here chain stems commonly undergo uniaxial rotational diffusions in the fast motional limit.[37,38] Such unique fast dynamics for PE in the hexagonal packing, 1,4-*trans*-polybutadiene in the high temperature phase, and form II of iPB are highly related to local structural disorders in both chain packing and conformation.

Compared with dynamic analyses in mobile crystals, there are very few results providing information about immobile polymer dynamics up to the melting point. English and coworkers[39] clarified that nylon does not show overall stem motions in the crystalline region up to its melting point. Nylon possesses NH and CO groups in a repeating unit and shows cooperative hydrogen bonding between stems. In addition, the repeating unit is much longer than in simple polyolefins. These two structural factors highly restrict the overall motions of the stems in nylon.[20,39] In contrast, iPB1 consists of (i) nonpolar hydrocarbons, (ii) short-length monomer units and (iii) regular helical conformations. These structures are common in similar polyolefins. Thus, only chain packing is a structural factor that restricts both the overall and the side-chain dynamics in form I. In particular, form I of iPB1 has very tight packing structures compared with other polyolefins.

On the basis of molecular dynamics, Hu and Schmidt-Rohr[20] categorized semi-crystalline polymers as either mobile crystals or fixed crystals. iPB1 achieves both extremely fast and slow-limit dynamics characteristics through a unique two-step process:

(i) crystallization into form II and (ii) an irreversible solid–solid transition into form I. We will further investigate how unique molecular dynamics in both forms influence the structures and properties of iPB1.

Mobility effects on lamellar thickness

Very recently, De Rosa *et al.*[33] reported that the low isotacticity sample directly crystallizes into form I′ from the melt state. Here the stereoregularity effects on lamellar thickness $\langle l \rangle$ were investigated. Figure 6a shows the $\langle l \rangle$–$1/\Delta T$ relation of two iPB1 samples with different stereoregularity. iPB1 experiences crystallization into form II and a subsequent solid–solid transition into form I $\langle l \rangle$ was obtained following the solid–solid transition. This sample shows a very wide $\langle l \rangle$ range from 10 nm at T_c=50 °C to 28 nm at T_c=110 °C. The best fit to the experimental data provides a slope of $624 \pm 4\,\mathrm{nm\,K^{-1}}$. Low_iPB1 directly crystallizes into form I′. The $\langle l \rangle$–$1/\Delta T$ relation shows a different line with a null slope of $32 \pm 3\,\mathrm{nm\,K^{-1}}$. The $\langle l \rangle$ range is only 4.6–5.3 nm. Therefore, two samples show largely different $1/\Delta T$ dependencies of $\langle l \rangle$.

Two possible mechanisms might contribute to the largely different slopes in the $\langle l \rangle$–$1/\Delta T$ relation for the two samples. One is a purely chemical effect on $\langle l \rangle$. Another is a physical mobility effect in different crystalline forms. There are several works addressing the chemical effects with regard to the lamellar thickness of semi-crystalline polymers.[40,41] Cheng *et al.*[40] investigated the effects of stereoregularity ($\langle mmmm \rangle$=78–99%) on the $\langle l \rangle$ of iPP at various T_cs. We replotted their results in addition to a recent result on the $\langle l \rangle$ of iPP[19] over a wide temperature range in Figure 6b. The low isotacticity samples show thinner lamellar thickness than do those of high isotacticity. Nevertheless, the $\langle l \rangle$–$1/\Delta T$ relations of all of the samples are described in terms of one universal line. A similar result was obtained in *syndiotactic*-poly(propylene-octene) copolymers by Strobl.[41] These results indicate that chemical disorder influences $\langle l \rangle$ values, but does not change the slope of the universal line of $\langle l \rangle$–$1/\Delta T$. Thus, the largely different slopes of the two iPB1 samples must be attributed to a huge difference in mobility between forms I′ and II. Extremely fast dynamics in form II leads to large variations in $\langle l \rangle$ at different crystallization temperatures. In contrast, the direct crystallization of form I′ into a fixed crystal results in very thin lamellae with $\langle l \rangle$= approximately 5 nm. This small thickness is reasonably explained in terms of the immobility of the crystalline stems in form I′.

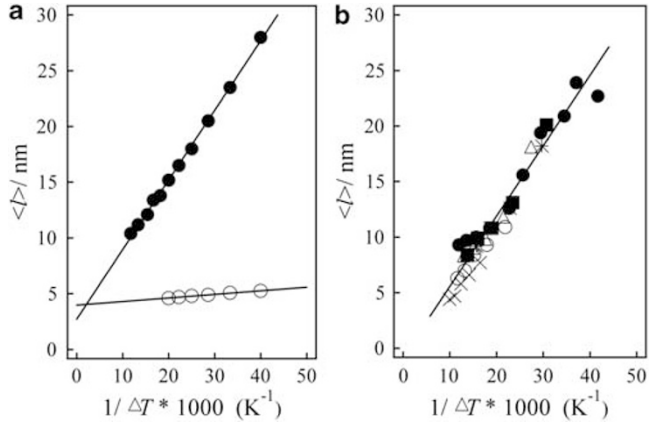

Figure 6 The $\langle l \rangle$–$1/\Delta T$ diagram of (**a**) *isotactic*-poly(1-butene) with $\langle mmmm \rangle$=92 (●) and 78% (○) and (**b**) *isotactic*-poly(propylene) with $\langle mmmm \rangle$=99 (■), 98 (Δ), 97 (●), 95 (*), 88 (○) and 78%, (×).

Polymorphism

Here we consider the polymorphism of forms I and I′. So far, several works have focused on the structural difference between forms I and I′. Among the previous characterizations, only DSC detected a large difference in the T_ms (T_m=130 °C for form I and 80–95 °C for form I′).[33,42] This result provided direct evidence that form I′ and I are different polymorphs. It was suggested from a large difference in their T_ms that form I′ is structurally disordered form I.[42] Molecular dynamics is quite sensitive to local environments. If structural disorders are included in form I′, significant molecular dynamics might be expected. Our current results, however, did not show any dynamics evidence in form I′ up to T_m or in form I. These local dynamics results are consistent with the static structures obtained using XRD, which indicated that both crystalline forms are the same trigonal crystals consisting of 3_1 helices.[33] These locally static and dynamic structures are not consistent with the structural views of form I′ using DSC. As shown above, there is a large difference in the $\langle l \rangle$ values between forms I and I′. The Gibbs-Thomson equation indicates that there is a strong correlation between T_m and $\langle l \rangle$. Thus, a large difference in melting points between forms I and I′ is reasonably explained in terms of a huge difference in $\langle l \rangle$ values. Form I is always produced after passing through the extremely mobile crystal, form II. In contrast, form I′ is formed by direct crystallization (bypassing form II). Thus, the huge mobility difference between forms I (I′) and II (>8 orders of magnitude) leads to largely different $\langle l \rangle$ and T_m values. In other words, there are different crystallization mechanisms that either pass through or bypass form II and lead to the observed large differences in the T_m and $\langle l \rangle$ values between forms I and I′.

Material properties

The mechanical properties of bulk samples are affected by crystallinity, lamellae thickness, morphology and chain mobility. Here we explain how (i) a unique crystallization into form II and (ii) the subsequent solid–solid transition into form I results in the superior material properties of iPB1. As discussed above, crystallization into form II leads to very thick lamellae at low supercooling (for example, $\langle l \rangle$=28 nm at ΔT=25 °C). In contrast, direct crystallization into immobile crystals (form I′) results in very thin lamellae with $\langle l \rangle$= approximately 5 nm. This means that immobile crystals cannot produce thick lamellae. The two step process of (i) crystallization into an extremely mobile mesophase and (ii) an irreversible solid–solid transition into the immobile crystal of form I is the only way to produce very thick lamellae for immobile crystals. Subsequently, storage at ambient temperature induces 'irreversible' solid–solid transitions from the metastable form II into the stable form I. Azzurri *et al.* reported that forms II–I transitions do not change the lamellar thickness or the crystallinity.[13] Form I crystals preserve the lamellae thickness and crystallinity that is induced by extremely high chain mobility in form II, depending on the crystallization temperature. As explained above, form I is a fixed crystal, which is largely different from the similar polyolefins PE,[16] iPP[17,18] and iP4M1P[19] (mobile crystals). There is a strong correlation between thermally activated molecular dynamics in the crystalline regions and dissipation of the bulk mechanical property.[16] Thus, Hu and Schmidt-Rohr[20] indicated that local overall dynamics in the crystalline regions are the origin of reduction of the bulk mechanical property and the drawability. The absence of molecular dynamics in form I can reasonably explain the superior mechanical properties and low drawability of iPB1 even at very high temperatures.[1,43] Direct crystallization into form I′ also leads to a fixed crystal. However, thin lamellae thickness leads to low melting temperatures. Therefore, it is concluded that only the two-

step process of (i) unique crystallization and (ii) an irreversible solid–solid transition leads to high crystallinity, thick crystal lamellae and the superior mechanical properties of iPB1.

CONCLUSION

In this work, it was demonstrated that both forms I and II of iPB show unique molecular dynamics when compared with other semi-crystalline polymers. Form II shows continuous rotational diffusion along with side-chain conformational transitions in the fast motional limit ($\langle \tau_c \rangle < 10^{-7}$ s) at 100 °C. This is direct evidence that form II is a conformationally disordered crystal. Following the irreversible solid–solid transition, the crystalline stems in form I do not undergo any overall or side-chains dynamics up to the melting point in the slow motional limit ($\langle \tau_c \rangle > 10$ s). This immobility was reasonably explained in terms of densifications of the crystalline regions. These huge dynamic contrasts have critical roles for both the structural organization and the material properties of iPB1. Extremely fast dynamics easily leads to very thick lamellae at very high temperatures. Following the solid–solid transition, the immobility of the crystalline stems in thick lamellae is a reason for the maintained bulk mechanical strength at very high temperatures. Comparison of local dynamics in iPB1 with those in similar polyolefins can reasonably explain why only iPB1 shows superior mechanical properties among polyolefins.

1 Gedde, U. W., Viebke, J., Leijström, H. & Ifwarson, M. Long term properties of hot-water polyolefin pipe-a review. *Polym. Eng. Sci.* **34,** 1773–1787 (1994).
2 Natta, G., Corradini, P. & Bassi, I. W. Crystal structure of isotactic poly-alpha-butene. *Nuov. Chim. Suppl.* **15,** 52–67 (1960).
3 Turner-Jones, A. Polybutene-1-type II crystalline form. *J. Polym. Sci. Part B* **1,** 455–456 (1963).
4 Petraccone, V., Pirozzi, B., Frasci, A. & Corradini, P. Polymorphism of isotactic poly-α-butene conformational analysis of the chain and crystalline structure of form 2. *Eur. Polym. J.* **12,** 323–327 (1976).
5 Cojazzi, G., Malta, V., Celotti, G. & Zannetti, R. Conformational flexibility of isotactic poly-1-olefins. *Makromol. Chem.* **177,** 915–926 (1976).
6 Tuner-Jones, A. Cocrystallization in copolymers of α-olefins II-butene-1 copolymers and polybutene type II/I crystal phase transition. *Polymer* **7,** 23–59 (1966).
7 Gohil, R. M., Milles, M. J. & Petermann, J. On the molecular mechanism of the crystal transition (tetragonal-hexagonal) in polybutene-1. *J. Macromol. Sci. Phys.* **B21,** 189–201 (1982).
8 Nakamura, K., Aoike, T., Usaka, K. & Kanamoto, T. Phase transformation in poly(1-butene) upon drawing. *Macromolecules* **32,** 4975–4982 (1999).
9 Maruyama, M., Sakamoto, Y., Nozaki, K., Yamamoto, T., Kajioka, H., Toda, A. & Yamada, K. Kinetic study of the II-I phase transition of isotactic polybutene-1. *Polymer* **51,** 5532–5538 (2010).
10 Lotz, B., Mathieu, C., Thierry, A., Lovinger, A. J., De Rosa, C., Ruiz de Ballesteros, O. & Auriemma, F. Chirality constraints in crystal-crystal transformations: isotactic poly(1-butene) versus syndiotactic polypropylene. *Macromolecules* **31,** 9253–9257 (1998).
11 Meng, Y. & Rieger, J. Synchrotoron ultrasmall-angle X-ray scttering studies on tensile defroamtion of poly(1-butene). *Macromolecules* **37,** 9481–9488 (2004).
12 Tosaka, M., Kamijo, T., Tsuji, M., Kohjiya, S., Ogawa, T., Isoda, S. & Kobayashi, T. High-resolution transmission electron microscopy of crystal transformation in solution-grown lamellae of isotactic polybutene-1. *Macromolecules* **33,** 9666–9672 (2000).
13 Azzurri, F., Flores, A., Alfonso, G. C., Sics, I., Hsiao, B. S. & Balta Calleja, F. J. Polymorphism of isotactic polybutene-1 as revealed by microindentation hardness. Part II: correlations to microstructure. *Polymer* **44,** 1641–1645 (2003).
14 Di Lorenzo, M. L., Righetti, M. C. & Wunderlich, B. Influence of crystal polymorphism on the three-phase structure and on the thermal properties of isotactic poly(1-butene). *Macromolecules* **42,** 9312–9320 (2009).
15 Schmidt-Rohr, K. & Spiess, H. W. *Multidimensional Solid-State NMR and Polymers* (Academic Press, London, 1994).
16 Hu, W. G., Boeffel, C. & Schmidt-Rohr, K. Chain flips in polyethylene crystallites and fibers characterized by dipolar C-13 NMR. *Macromolecules* **32,** 1611–1619 (1999).
17 Schaefer, D., Spiess, H. W., Suter, U. W. & Fleming, W. W. Two-dimensional solid-state NMR studies of ultraslow chain motion: glass transition in atactic poly(propylene) versus helical jumps in isotactic poly(propylene). *Macromolecules* **23,** 3431–3439 (1990).
18 Miyoshi, T., Mamun, A. & Hu, W. Molecular ordering and molecular dynamics in isotactic-poly(propylene) characterized by SS-NMR. *J. Phys. Chem. B* **114,** 92–100 (2010).
19 Miyoshi, T., Pascui, O. & Reichert, D. Slow chain dynamics in isotactic-poly(4-methyl-1-pentene) crystallites near the glass transition temperature characterized by solid-state C-13 MAS exchange NMR. *Macromolcules* **37,** 6460–6471 (2004).
20 Hu, W- G. & Shimidt-Rohr, K. Polymer ultradrawability: the crucial role of α-relaxation chain mobility in the crystallites. *Acta. Polym.* **50,** 271–285 (1999).
21 Belfiore, A. A., Schiling, C. A., Tonelli, A. E., Lovinger, A. J. & Bovey, F. A. Magic angle spinning carbon-13 NMR spectroscopy of three crystalline forms of isotactic-poly(1-butene). *Macromolecules* **17,** 2561–2565 (1984).
22 Maring, D., Meurer, B. & Weill, G. ^{1}H NMR Studies of molecular relaxations of poly-1-butene. *J. Polym. Sci. Part B* **33,** 1235–1247 (1995).
23 Maring, D., Whilhelm, M., Spiess, H. W., Meurer, B. & Weill, G. Dynamics in the crystalline polymorphic forms I and II and III of isotactic poly-1-butene. *J. Polym. Sci. Part B* **38,** 2611–2624 (2000).
24 Beckham, H. W., Schmidt-Rohr, K. & Spiess, H. W. conformational disorder and its dynamics within the crystalline phase of the form II polymorph of isotactic poly(1-butene). *ACS Symp. Ser.* **598,** 243–253 (1995).
25 Miyoshi, T., Hayashi, S., Imashiro, F. & Kaito, A. Side-chain conformation and dynamics for the form II polymorph of isotactic poly(1-butene) investigated by high-resolution solid-state C-13 NMR spectroscopy. *Macromolecules* **35,** 6060–6063 (2002).
26 Miyoshi, T., Mamun, A. & Reichert, D. Fast dynamics and conformations of polymer in a conformational disordered crystal characterized by ^{1}H-^{13}C WISE NMR. *Macomoelcules* **43,** 3986–3989 (2010).
27 Miyoshi, T., Hayashi, S., Imashiro, F. & Kaito, A. Chain dynamics, conformations, and phase transformations for form III polymorph of isotactic poly(1-butene) investigated by high-resolution solid-state C-13 NMR spectroscopy and molecular mechanics calculations. *Macromolecules* **35,** 2624–2632 (2002).
28 Wunderlich, B., Moller, B., Grebowicz, J. & Baur, H. conformational motion and disorder in low and high molecular mass crystals. *Adv. Polym. Sci.* **87,** 1 (1988).
29 deAzevedo, E. R., Hu, W. G., Bonagamba, T. J. & Schmidt-Rohr, K. Centerband-only detection of exchange: efficient analysis of dynamics in solids by NMR. *J. Am. Chem. Soc.* **121,** 8411–8412 (1999).
30 Schmidt-Rohr, K., Clauss, J. & Spiess, H. W. Correlation of structure, mobility, and morphological information in heterogeneous polymer materials by 2-dimensional wideline-separation NMR-pectroscopy. *Macromolecules* **25,** 3273–3277 (1992).
31 Tekely, P., Palmas, P. & Mutzenhardt, P. Elimination of heteronuclear dipolar interaction effects from C-13 detected proton spectra in wideline separation nuclear magnetic-resonance spectroscopy. *Macromolecules* **26,** 7363–7365 (1993).
32 Qiu, X. & Mirau, A. P. WIM/WISE NMR studies of chain dynamics in solid polymers and blends. *J. Magn. Reson.* **142,** 183–189 (2000).
33 De Rosa, C., Auriemma, F., deBallesteros, O. R., Exposito, F., Laguzza, D., Girolamo, R. D. & Resconi, L. Crystallization properties and polymorphic behaviors of istactic poly(1-butene) from metallocene catalysts: the crystallization of form I from the melt. *Macromolecules* **42,** 8286–8297 (2009).
34 Takahashi, T., Kawashima, H., Sugisawa, H. & Baba, T. ^{207}Pb chemical shift thermometer at high temperature for magic angle spinning experiments. *Solid State NMR* **15,** 119–123 (1999).
35 Nakai, T., Ashida, J. & Terao, T. Determination of the ^{13}C chemical shift tensors in isotactic polypropylene via the two-dimensional powder pattern in rotating solids. *Magn. Reson. Chem.* **27,** 666–668 (1989).
36 Liu, S. F., Mao, J. D. & Schmidt-Rohr, K. A robust technique for two-dimensional separation of undistorted chemical-shift anisotropy powder patterns in magic-angle-spinning NMR. *J. Magn. Reson.* **155,** 15–28 (2002).
37 de Langen, M. & Prins, K. O. Mobility of polyethylene chains in the orthorhombic and hexagonal phases investigated by NMR. *Chem. Phys. Lett.* **299,** 195–200 (1999).
38 Möller, M Structure and dynamics of the high temperature polymorph of *trans*-1,4-polybutadiene. *Macromol. Chem. Rapid Commun.* **9,** 107–114 (1988).
39 Hirschinger, J., Miura, H., Gardner, K. H. & English, A. D. Segmental dynamics in the crystalline phase of nylon 66: solid state deuterium NMR. *Macromolecules* **23,** 2153–2169 (1990).
40 Cheng, S. Z. D., Janimak, J. J., Zhang, A. & Hsieh, E. T. Isotacticity effect on crystallization and melting in polypropylene fractions: 1. Crystalline structures and thermodynamic property changes. *Polymer* **32,** 648–655 (1991).
41 Strobl, G. Colloquium: laws controlling crystallization and melting in bulk polymers. *Rev. Mod. Phys.* **81,** 1287–1330 (2009).
42 Boor, J. Jr & Youngman, E. A. Polymorphism in poly(1-butene): apparent direct formation of modification I. *J. Polym. Sci. Patr B* **2,** 903–907 (1964).
43 Sawai, D., Anyashiki, T., Nakamura, K., Hisada, N., Ono, T. & Kanaoto, T. Ultradrawing above the static melting temperature of ultra-high molecular weight isotactic poly (1-butene) having low ductility in the crystalline state. *Polymer* **48,** 363–370 (2007).